GENETIC MONITORING OF THE RIO GRANDE SILVERY MINNOW: GENETIC STATUS OF WILD AND CAPTIVE STOCKS IN 2021

Annual report FY 2021

Megan J. Osborne and Thomas F. Turner
Department of Biology and Museum of Southwestern Biology MSC 03-2020,
University of New Mexico New Mexico, 87131, USA

Agreement: R19AP00025

Submitted to:
Jennifer Bachus and Eric Gonzales
U. S. Bureau of Reclamation-UC-AAO
Albuquerque, New Mexico.
15th November 2021

Table of contents

List of Tables and Figures

EXECUTIVE SUMMARY

Genetic monitoring of the middle Rio Grande population of Rio Grande Silvery Minnow (*Hybognathus amarus*) has been conducted annually from 1999-2012 and 2014-2021. This work includes monitoring stocks that were bred or reared in captivity and released to the Rio Grande in New Mexico. Genetic monitoring of captive stocks commenced in 2002; marking the commencement of the augmentation program. In 2021, genetic monitoring was based on genotyping 239 'wild' Rio Grande Silvery Minnow collected from all three occupied reaches of the middle Rio Grande (Table 1 and Table 2), as well as progeny of captive stocks from Southwestern Native Aquatic Resources and Recovery Center (Southwestern ARRC), Albuquerque Biological Park and the Los Lunas Silvery Minnow Refugium (LLSMR). These fish represent the potential breeding population in 2021. We also genotyped broodstocks held at Southwestern ARRC (YC2020), Albuquerque Biological Park (YC2016, YC2019, YC2020) and from the LLSMR (YC2019, YC2020).

Major findings for 2021

(1) Gene diversity and allelic diversity were similar to values recorded in 2020 (Table 3, Figure 1). Observed heterozygosity was the lowest value seen since 2010; this means that more individuals had identical alleles at microsatellite loci than in more recent years (2011-2020). Increased homozygosity can be an indication of increased matings between related individual (that share alleles). At the reach level, allelic diversity and gene diversity were virtually identical between the Angostura, Isleta and San Acacia reaches and diversity measures were all above benchmark values (Figure 2). Heterozygosity was lower in the Angostura and Isleta reaches compared to the San Acacia reach and was also lower than values recorded in 2020.

(2) In 2021, mitochondrial (mtDNA) haplotype richness (number of haplotypes adjusted to account for differences in sample size between collections) decreased over 2020 values while gene diversity increased. However, both diversity metrics remained within the range seen across the time series (Table 3, Figure 3). Across all 2021 samples (including hatchery collections) ten haplotypes were detected including two rare haplotypes (I and V) (Table 3); ten haplotypes were also detected in 2018, 2019 and 2020. Among wild collections in 2021, only eight haplotypes were detected and for the first time since 1999, we did not detect haplotype E.

(3) Genetic effective population size estimates based on changes in allele frequencies from one year to the next (N_{eV}) reveal a substantial decline in 2021 (Table 2, Figures 6-8) with N_{eV} and N_{ef} estimates among the lowest values (<100) since genetic monitoring began. Specifically, the genetic effective size estimate based on microsatellites was N_{eV}=62 for the 2020-2021 comparison compared to N_{eV}=425 for 2019-2020 period. For the 2020-2021 temporal comparison, N_{ef} varied from N_{ef} = 56 - 69 depending on the estimation method used. Likewise, linkage disequilibrium effective size (which refers to the effective size of the parental population of the sample) (N_{eD}=1263) decreased from values in 2020 (N_{eD}=1927). These results are consistent with substantially reduced density (-88.8%) of Rio Grande Silvery Minnow in 2020 compared to 2019 (Dudley et al. 2021).

(4) To augment the wild population in fall 2020, 218,500 fish were released to the Rio Grande population. We genotyped representatives from three captive lots, including one lot from each hatchery facility (Southwestern ARRC, Albuquerque BioPark and LLSMR). Pooled hatchery samples released to the middle

Rio Grande in fall 2020 had levels of genetic diversity measured across microsatellite loci that were very similar to the 'wild' population in 2021 with the exception of observed heterozygosity which was reduced in the wild sample (Table 2). Across hatchery stocks released in 2020, total number of haplotypes and global haplotype richness were higher than in the wild population (Table 3). The fewest haplotypes and lowest haplotype diversity were seen in the fish released from the Albuquerque BioPark.

(5) Broodstocks from Southwestern ARRC, Albuquerque BioPark and the LLSMR were also genotyped in 2021. These samples represent the 2020 year classes (YC) held at Southwestern ARRC as well as the 2016, 2019 and 2020 year classes held at the Albuquerque BioPark, and 2019 and 2020 year classes from the LLSMR. Genetic diversity based on microsatellites and mtDNA of these broodstocks were within the range seen in the wild population. Three broodstock samples (BioPark YC19/YC20 and Southwestern ARRC YC20) contained 10 haplotypes detected in the wild population in previous years. Genetic diversity in the refugial broodstocks will be largely dependent upon the strength of the year class from which it was sourced. Finite genetic effective size estimated using the linkage disequilibrium method ranged from 1072 (LLSMR YC20) to 3255 (ABP YC20) across facilities (Table 2). This estimate pertains to effective size of the generation preceding the current sample.

INTRODUCTION

Genetic monitoring is defined as a collection of two or more temporally spaced genetic samples from the same population (Schwartz et al. 2007). Such studies typically employ neutral genetic markers and occasionally maternally inherited mtDNA, to track changes in standard genetic diversity metrics (gene diversity [H_e], heterozygosity [H_o], allelic richness [A_R] and genetic effective size [N_e]) over a contemporary time series (see glossary). It is widely recognized that erosion of genetic diversity increases a species' vulnerability to decline through lowered fitness (e.g., associated with inbreeding depression) that can ultimately accelerate a species' path to extinction. This is the rationale for tracking these metrics of diversity across time (e.g., Frankham 2005). The time scale of genetic monitoring varies considerably among studies from sampling over only a few years to the use of archival samples for a monitoring program that may span decades. In studies that encompass multiple decades, sampling is rarely conducted on an annual basis so linking changes in diversity metrics with specific environmental or management actions may not be plausible. In fish, genetic monitoring to date has been confined largely to marine species and freshwater salmonids. The genetic data that we have collected for Rio Grande Silvery Minnow spans a 34-year period (1987, 1999-2012, 2015-2021) and represents one of the longest genetic monitoring time series for a non-salmonid freshwater fish.

For genetic monitoring programs, empirical measurements of diversity and genetic effective size are typically obtained from neutrally-evolving microsatellite loci. Microsatellites are short tandemly repeating DNA sequences that are found throughout the genome of most species (reviewed in Dowling et al. 1996). They are bi-parentally inherited and are highly polymorphic among individuals (which is particularly important for endangered species that may have limited genetic diversity) and hence are the most widely used genetic markers in molecular ecology and conservation genetics studies. MtDNA is a haploid marker (i.e., individuals only have one copy as opposed to two copies for microsatellites), so progeny inherit a single mtDNA molecule from the female parent only. Due to differences in how nuclear DNA and mtDNA are inherited, they provide complementary approaches to monitoring genetic diversity.

The Rio Grande Silvery Minnow is a small-bodied (<90 mm standard length), short-lived (in the spring the vast majority of fish are age-1; Horwitz et al. 2018) cyprinid. This species was historically widely distributed in the Rio Grande from northern New Mexico to the Gulf of Mexico, and in the Pecos River from northern New Mexico to the confluence of the Rio Grande in Texas (Pflieger 1980). Habitat changes associated with river fragmentation caused by water storage dams and diversion structures and changes to the natural hydrograph have resulted in significant range contraction. The interaction of these factors with species life-history causes changes in population density that can span several orders of magnitude from one year to the next (Dudley et al. 2021). Over the past 20-years, periodic droughts and resulting channel dewatering have caused recruitment failure in some years and periodic population collapse (Archdeacon et al. 2020a). Today a remnant population persists in the highly fragmented and regulated Rio Grande in New Mexico. This 280-km river segment represents less than 5% of the historical range of the species and extends from downstream of Cochiti Dam to Elephant Butte Reservoir. This stretch of river is bisected by three water diversion structures that define distinct river reaches (from north to south: Angostura, Isleta, and San Acacia). Rio Grande Silvery Minnow was listed under the Endangered Species Act in 1994 (U.S. Fish and Wildlife Service 1994). This species is now intensively managed including a captive breeding program and annual augmentation of the Rio Grande population that has been in place since 2003 (U.S. Fish and Wildlife Service 2018).

The Rio Grande Silvery Minnow population is sampled annually throughout its current range, using nine microsatellite loci and a mtDNA gene to measure the trajectory of genetic diversity measured by allelic richness, heterozygosity, and genetic effective population size. The temporal component and sampling strategy provide the framework necessary to examine impacts of changes in abundance, management actions and environmental conditions on genetic diversity at these loci. Negative genetic impacts to a population can occur over relatively short time periods for fishes characterized by a short lifespan (the population is dominated by age-1 fish in the spring; Horwitz et al. 2018) and in which dramatic changes in abundance occur from year to year. As such, genetic monitoring is a crucial component to management of Rio Grande Silvery Minnow. Here, we report on the genetic status of the population in 2021 and compare these results to previous years.

MATERIALS AND METHODS

Sampling- Rio Grande population

Throughout this study, we use the term 'wild' to refer to unmarked fish sampled directly from the Rio Grande, as opposed to individuals tagged with a Visible Implant Elastomer (VIE) tag to indicate that they were reared in a hatchery and used to supplement the Rio Grande Silvery Minnow population. We use the term 'wild caught hatchery' (WCH) to refer to individuals with a VIE tag. 'Wild' fish may have parents that were wild or bred/reared in captivity, but were hatched in the Rio Grande. Unmarked (n=426) Rio Grande Silvery Minnow were collected between October 29th and December 15th 2020; these are assumed to represent the potential breeding population in 2021. These samples add to the data collected from wild Rio Grande Silvery Minnow sampled from the middle Rio Grande annually from 1999 to 2012 and 2014-2019 (between November and April- just prior to reproduction) as well as 43 individuals used in a previous allozyme study of *Hybognathus* and stored in the Museum of Southwestern Biology Division of Genomic Resources (Cook et al. 1992 - referred to as 1987 sample). The distinction is made between 'wild' and WCH

fish for this reason and because population monitoring tracks 'wild' fish separately from hatchery released fish. Collections were made throughout the current distribution (i.e., from Cochiti reservoir to Elephant Butte reservoir in New Mexico) of Rio Grande Silvery Minnow, with the exception of the Cochiti reach because the species is rare or absent in that area (Bestgen and Platania 1991). In 2021, wild fish were collected from all occupied river reaches by seining a variety of habitats in the Angostura (n=118), Isleta (n=60) and San Acacia (n=61) reaches (Table 1, Table 2). Collections were made roughly two months earlier than normal so as to avoid collection of untagged hatchery released fish. Fish were anesthetized in river water treated with MS-222 (Tricaine methane sulfonate 200 mg/L river water) at the site of capture. A piece of caudal fin was removed from each individual. Fin clips were preserved in 95% ethanol.

Sampling- Captive lots and Broodstock

In 2021, fin clips representing fish released in fall 2020 from Southwestern ARRC (n=101), Albuquerque BioPark (n=48) and LLSMR (n=100) were genotyped. We also genotyped broodstocks held at Southwestern ARRC (2020 n=199), Albuquerque Biological Park (YC 2016 n=98; YC 2019 n=199; YC 2020 n=258) and the LLSMR (YC 2019 n=50; YC 2020 n=149).

Table 1. Sample sizes and collection localities of wild Rio Grande Silvery Minnow by river reach for samples collected during 2021 genetic monitoring.

Angostura	
Downstream of Alameda Bridge Crossing	44
Montano Bridge Crossing	14
Central Avenue bridge crossing (US HWY 66)	50
Rio Bravo Bridge Crossing	1
Avenida Cesar Chavez Bridge Crossing	9
Isleta	
Rio Grande west of Lagrima Rd	56
Ca. 1.0 mi upstream of NM State HWY 309 bridge crossing, Belen.	2
Ca. 1.2 mi upstream of San Acacia Diversion Dam, San Acacia.	1
Upstream of NM State HWY 6 bridge crossing, Los Lunas.	1
San Acacia	
Escondida	9
San Acacia Diversion Dam	48
Ca. 1.5 mi downstream of San Acacia Diversion Dam	3
Ca. 4.5 miles upstream of US Hwy 380 Bridge Crossing, San Antonio	1
Grand Total	239

Table 2. All 'wild' samples collected from the middle Rio Grande by river reach for 1987, 1999-2012 and 2014-2021.

*Genetic analysis was not conducted in 2014 due to the small number of samples collected.

Year	Angostura	Isleta	San Acacia	Total
1987	15	-	28	43
1999	-	-	46	46
2000	-	-	194	194
2001	-	65	63	128
2002	67	121	201	389
2003	71	65	33	169
2004	141	15	6	162
2005	190	109	95	394
2006	95	143	145	383
2007	48	128	42	218
2008	165	191	123	479
2009	175	153	150	478
2010	149	146	151	446
2011	71	148	140	359
2012	147	215	154	516
2013	-	-	-	-
2014*	5	3	4	12
2015	75	33	35	143
2016	171	121	128	420
2017	159	156	154	469
2018	152	148	143	443
2019	73	10	54	137
2020	148	127	151	426
2021	118	60	61	239

Molecular methods- microsatellites

Total nucleic acids, including genomic and mitochondrial DNA were extracted from air-dried fin clips using proteinase-K digestion and organic extraction methods (Hillis et al. 1996). Individuals were genotyped at nine microsatellite loci: *Lco1*, *Lco3*, *Lco6*, *Lco7*, *Lco8* (Turner et al. 2004); *Ca6* and *Ca8* (Dimsoski et al. 2000); and *Ppro118* and *Ppro126* (Bessert and Orti 2003). The following pairs of loci were amplified through multiplex PCR: *Lco1*/*Ca6* and *Lco6*/*Lco7* (1X PCR buffer, 3 mM $MgCl_2$, 125 micromol [μM] deoxyribonucleotide triphosphates [dNTPs], 0.40-0.50 μM each primer, 0.375 units *Taq* polymerase); *Lco3* and *Lco8* (1X PCR buffer, 2 mM $MgCl_2$, 0.8 mM dNTPs, 0.40-0.50 μM each primer, 0.375 units *Taq*); and *Ppro 118*/*Ppro126* (1X PCR buffer, 3 mM $MgCl_2$, 0.8 mM dNTPs, 0.40-0.50 μM each primer, 0.375 units *Taq*). *Ca8* was amplified alone (1X PCR buffer, 3 mM $MgCl_2$, 0.8 mM dNTPs, 0.50μM each primer, 0.375 units *Taq* polymerase). PCR cycling conditions for all loci were as follows: one denaturation cycle of 92°C for 2 min followed by 30 cycles of 90 °C for 20s, 50°C for 20 s, 72°C for 30s. Cycling conditions for *Ppro 118*/*Ppro126* were as follows: one denaturation cycle of 92°C for 2 min followed by 30 cycles of 90 °C for 20s, 60°C for 20 s, 72°C for 30s. Primer concentrations in multiplex reactions were optimized by locus to ensure equal amplification each microsatellite. Fragment size analysis on an ABI 3130 automated capillary sequencer was performed by combining 1 μl of PCR product with 10 μl of formamide and 0.4 μl of HD400 size standard and denatured at 93°C for 5 minutes. Genotype data were scored in GENEMAPPER Version 4.0 (Applied Biosystems). In addition, to genotyping the samples collected in 2021, we also reisolated DNA and regenotyped samples collected in 1999 to reduce the amount of "missing" data in this collection.

MtDNA- ND4

A 295-base pair (bp) fragment of the mtDNA ND4 gene was amplified from each individual in a 10 μL reaction containing 1 μL template DNA, 1 μL 10× reaction buffer, 2 mM $MgCl_2$, 0.8 μM dNTPs, 0.5 μM forward (5'- GAC CGT CTG CAA AAC CTT AA- 3') and reverse primer (5'- GGG GAT GAG AGT GGC TTC AA – 3'), and 0.375 units *Taq*. PCR conditions were 90° C initial denaturation for 2 minutes followed by 30 cycles of 90° C for 30 seconds, 50° C for 30 seconds, and 72◦ C for 30 seconds. Sequence data was obtained for all individuals by direct sanger sequencing (Big Dye vers. 1.1) according to the manufacturer's instructions and using an ABI 3130 DNA Sequencer.

Statistical analysis

GENEPOP'007 (Rousett 2008) was used to test for departures from Hardy-Weinberg equilibrium (HWE), using the procedure of Guo and Thompson (1992) and to perform global tests for linkage disequilibrium for all pairs of loci in each collection. Sequential Bonferroni correction (Rice 1989) was applied to account for inflated Type-1 error rates associated with multiple simultaneous tests. In some cases, sample sizes differed between collections, particularly between some samples collected early in the study and more recent collections. The number of alleles and heterozygosity are dependent on sample size, so we used a resampling approach to correct for sample size effects on diversity measures and make them more comparable across collections. In short, we randomly sampled each collection without replacement using the minimum sample size across all years (n = 43 in 1987). Microsatellite diversity estimates (corrected number of alleles [N_{AC}], Nei's (Nei 1987) gene diversity [H_{EC}] and heterozygosity [observed proportion of heterozygotes] [H_{OC}]) were then calculated for the random sample and the process repeated for 1000 iterations. Corrected diversity estimates are calculated as the mean estimate across all iterations. This analysis was conducted in the R statistical package (www.r-project.org). This resampling technique was also used for comparisons among collections obtained across years and river reaches, we repeated the resampling procedure for microsatellite

data with diversity measures based on n=15 (1987, San Acacia) and excluding the smallest samples (2004 San Acacia; Isleta 2019). For each microsatellite locus and population, inbreeding coefficients (F_{IS}) were obtained using the R statistical package *hierfstat* vers. 0.5-7 (Goudet and Jombart 2015, 2020).

Mitochondrial diversity was characterized by number of haplotypes (N_h), haplotype diversity (*h*), and haplotype richness (H_R). These metrics are roughly equivalent to the number of alleles, gene diversity (H_{EC}), allelic diversity (N_{AC}) averaged across microsatellite loci. Haplotype richness (H_R) (Petit et al. 1998) was obtained using the R package *hierfstat* vers. 0.5-7 (Goudet and Jombart 2020). Haplotype diversity (*h*) is a measure of the uniqueness of a haplotype in a population. Values of *h* range from zero (all individuals have the same haplotype) to one (all individuals have a different haplotype). The calculation of *h* is based on the sample size and the frequency of each haplotype in the population.

To place levels of diversity across years in context of overall genetic diversity of the species and to develop a biologically relevant benchmark for assessing levels of diversity within samples, we used an additional resampling technique. All 'wild' fish were pooled into one large population (n = 6671) from which we iteratively took samples (n = 43 by year; n=15 by reach benchmarks) to estimate diversity statistics. Our primary interest is maintaining genetic diversity, hence we estimated a one-tailed lower 95% confidence intervals that corresponds to the upper 95% of the resampled distribution (i.e., 9500 of 10000 iterations). Thus, the distribution contained within this confidence interval corresponds to the null hypothesis of no loss of diversity.

F-statistics

Weir and Cockerham's (1984) *F*-statistics (microsatellites) and *Φ*-statistics (mtDNA) were calculated in the R package *diveRsity* vers 1.9 (Keenan 2017) and Arlequin ver. 3.11 (Excoffier et al. 2005), respectively. Hierarchical analysis of molecular variance (AMOVA) was used to test whether a significant proportion of genetic variance was partitioned into components attributable to differences among 'wild', captive-spawned, and broodstock fish (F_{CT}, Φ_{CT}), among samples within these three groups sampled in 2021 (F_{SC}, Φ_{SC}) and among all samples (F_{ST}, Φ_{ST}). P-values for all statistics were generated using bootstrapping (9999 permutations). We calculated pairwise F_{ST} values between all temporal samples collected from the Rio Grande. Upper and lower 95% CIs were obtained using bootstrapping (1000 permutations) implemented in the R package *diveRsity*.

Estimation of genetic effective size

Variance effective size (N_{eV}) and 95% confidence intervals (CIs) were estimated from annual changes in microsatellite allele frequencies across annual samples, using the temporal methods of Nei and Tajima (1981) and Jorde and Ryman (2007), implemented in NEESTIMATOR vers 2.1 (Do et al. 2014). Highly polymorphic loci with many rare alleles, typical of microsatellites, can result in biased estimates of N_{eV} (Hedrick 1999; Turner et al. 2001). To minimize this bias, we used the P_{CRIT} value 0.02 to exclude low frequency alleles. Rio Grande Silvery Minnow were sampled under Plan I (prior to reproduction, with replacement) for all methods. The parametric method was used to calculate 95% confidence intervals. Multiple temporal methods are used to calculated N_{eV} to ensure consistency across estimators. Additionally, N_{eV} was estimated using the pseudo-maximum-likelihood (MLNE) method implemented in the program MLNE (Wang and Whitlock 2003).

For all methods, we assumed that immigration (except from hatchery stocks) from outside the study area did not affect estimates of N_e. We equated the number of years separating a pair of samples with the number of generations elapsed between samples because Rio Grande Silvery Minnow have essentially non-overlapping generations (based on unpublished population monitoring data of R. K. Dudley and S. P. Platania). However, to account for small but known deviation from the discrete generation model (G = 1.27), we corrected consecutive estimates of N_{eV} and N_{ef} for overlapping generations (Turner et al. 2006; Osborne et al. 2010), using the analytical method of Jorde and Ryman (1995, 1996). In addition to consecutive pairwise estimates, we also present comparisons between the 1987 and 1999 samples to provide historical context for the contemporary estimates. As these samples (1987-1999) were collected more than 3-5 generations apart, the drift signal should be sufficiently large relative to sampling biases associated with age-structure such that correction for overlapping generations is unnecessary (Waples and Yokota 2007).

We used the linkage disequilibrium method (Hill 1981) that only requires a single temporal sample to estimate the linkage disequilibrium effective size (N_{eD}). Annual N_{eD} was estimated from microsatellite DNA data separately for 'wild', captive-spawned stocks, and broodstock samples using the updated version of the program NEESTIMATOR vers. 2.1 (Do et al. 2014). Single sample N_e methods (such as those provided by N_{eD}) yield an estimate of the effective number of parents that produced the progeny from which the sample is drawn, and most closely approximates the inbreeding effective size, N_{eI} (Laurie-Ahlberg and Weir 1979; Waples 2005). Confidence intervals were determined using the jack-knife procedure implemented in NeEstimator.

Variance effective size was also estimated for the female portion of the population using mtDNA haplotype frequencies. To distinguish between variance effective size based on microsatellite data (N_{ev}) we use the designation N_{ef} to represent mtDNA variance effective size. N_{ef} was estimated with temporal (aka 'moments' method) and pseudo-maximum-likelihood (MLNE) methods (Wang 2001). It is useful to estimate genetic effective size from mtDNA data because it provides information pertaining to the female portion of the population. For example, when very low estimates of N_{ef} are obtained it implies that relatively few females are making a genetic contribution to the population.

RESULTS

Microsatellites- genetic diversity

Characterization of microsatellite genotypes from the 2021 samples revealed two loci (*Ca6* and *Ppro126*) as the least variable, each with 9-10 alleles detected across samples. Locus *Ppro118* was the most variable with 60 alleles followed by *Lco1* with 39 alleles detected across 2021 collections. In 2021, tests for deviations from Hardy-Weinberg Proportions were significant for 30% of locus-by-site combinations (30/90) following sequential Bonferroni correction for multiple comparisons. The majority of significant departures occurred at four loci (*Lco7*, *Lco8*, *Ca8*, *Ppro118*). Analysis by MICRO-CHECKER (Van Oosterhout et al. 2004) found that presence of null alleles was the most likely explanation for an excess of homozygous individuals. Three loci (*Lco1*, *Lco6*, *Ca6, Ppro126*) conformed to Hardy-Weinberg expectations in all collections, *Lco3* and *Ca8* departed from expectations in one and four collections respectively. Across all collections, significant tests for genotypic disequilibrium occurred in five of 360 comparisons following sequential Bonferroni correction; four significant tests occurred in one captive stock released in 2020 from the LLSMR.

Table 3. Diversity statistics for microsatellites and mtDNA.
N is sample size, N_{AC} is average number of alleles across loci, H_{EC} is Nei's gene diversity, H_{OC} is observed heterozygosity, F_{IS} is inbreeding co-efficient, N_h is number of haplotypes, *h* is haplotype diversity, and H_R is haplotype richness. Linkage disequilibrium estimates of effective size, N_{eD}, are also given. Genetic monitoring was not conducted in 2013. Values from 2021 monitoring year are in bold for emphasis; Wild caught hatchery fish (WCH) were included in genetic monitoring beginning 2014.

	Microsatellites								mtDNA			
Wild-MRG	**N**	**N_{AC}**	**H_{EC}**	**H_{OC}**	**F_{IS}**	**N_{eD}**	**-95**	**+95**	**N**	**N_h**	**h**	**H_R**
1987	43	13.8	0.786	0.71	0.084	1142	73	∞	37	7	0.743	7
1999	46	15.1	0.824	0.676	0.188	∞	220	∞	44	5	0.427	4.82
2000	194	14.1	0.803	0.698	0.129	∞	9130	∞	124	6	0.392	4.35
2001	128	14.8	0.796	0.72	0.097	1313	331	∞	122	10	0.643	7.19
2002	389	14.5	0.782	0.681	0.125	1739	755	∞	387	9	0.63	5.23
2003	169	14.7	0.806	0.71	0.122	1282	366	∞	167	9	0.524	5.89
2004	162	14.7	0.809	0.738	0.092	515	279	2119	161	11	0.62	7.47
2005	394	14.7	0.805	0.725	0.104	2015	816	∞	396	10	0.612	6.65
2006	383	15.1	0.814	0.726	0.118	2313	946	∞	378	10	0.624	6.67
2007	218	15.1	0.835	0.723	0.144	4237	798	∞	218	10	0.579	6.36
2008	474	15	0.811	0.712	0.125	3578	1394	∞	466	11	0.571	6.36
2009	476	14.9	0.82	0.689	0.161	3490	1244	∞	472	12	0.59	6.61
2010	440	15	0.824	0.693	0.162	7758	1697	∞	433	9	0.641	7.01
2011	362	15.1	0.82	0.725	0.121	∞	3117	∞	359	11	0.634	6.74
2012	517	15.2	0.817	0.727	0.113	7954	1892	∞	522	10	0.659	6.71
2013	-	-	-	-	-	-	-	-	-	-	-	-
2014	12	-	-	-	-	-	-	-	-	-	-	-
2015	144	15.1	0.805	0.732	0.092	489	321	951	143	8	0.655	6.47
2016	420	15.1	0.812	0.727	0.106	1798	1081	4741	420	9	0.75	7.08
2017	469	14.6	0.811	0.720	0.118	2524	1388	10841	469	10	0.651	6.48
2018	443	14.8	0.815	0.720	0.119	3375	1638	∞	419	10	0.743	7.38
2019	134	14.3	0.808	0.736	0.092	1329	527	∞	134	8	0.677	6.63
2020	426	14.7	0.813	0.729	0.106	1927	1131	5627	426	10	0.707	7.28
2021	239	14.7	0.817	0.694	0.148	1263	723	4219	239	8	0.718	6.65
2021 Benchmark	--	14.8	0.800	0.679	--	--	--	--	--	--	--	--

Table 3. continued

Wild-caught hatchery	N	N_{AC}	H_{EC}	H_{OC}	F_{IS}	N_{eD}	-95	+95	N	N_h	h	H_R
2014	184	14.8	0.831	0.774	0.069	133*	101	184	182	6	0.61	3.87
2015	300	15.43	0.825	0.731	0.115	289	206	443	297	8	0.63	5.25
2016	111	14.23	0.813	0.706	0.144	128	99	173	107	7	0.69	4.61
2019	127	14.00	0.807	0.693	0.145	327	172	1508	127	9	0.68	5.59
Captive spawned												
Global 2016 hatchery	**492**	**14.73**	**0.821**	**0.726**	**0.125**	**290**	**184**	**520**	**494**	**9**	**0.748**	**5.23**
ABP13-003-04 WC	50	13.8	0.808	0.702	0.134	407	190	∞	50	5	0.751	5.00
ABP16-003 CS	39	12.9	0.83	0.743	0.114	79	50	161	39	5	0.533	5.00
Uvalde 2016	100	12.1	0.789	0.700	0.113	47	36	62	100	7	0.745	5.17
16CSDX-003	100	13.2	0.801	0.724	0.102	104	80	141	100	6	0.766	6.10
16CSDX-004	98	10.6	0.801	0.743	0.076	30	25	37	98	6	0.710	5.28
16CSDX-005	100	12.1	0.796	0.732	0.086	55	41	75.4	100	6	0.716	5.09
Global 2017 hatchery	**484**	**13.8**	**0.812**	**0.725**	**0.111**	**179**	**120**	**284**	**484**	**10**	**0.736**	**5.08**
ABP	50	12.4	0.798	0.662	0.182	31	23.7	41	47	3	0.539	3.00
17CSDX-001	98	12.7	0.819	0.721	0.12	171	119	284	98	5	0.710	4.66
17CSDX-002	99	12.8	0.822	0.729	0.116	184	121	753	98	5	0.664	4.82
17CSDX-003	103	13	0.801	0.757	0.055	491	232	∞	102	6	0.707	5.41
17CSDX-004	99	13.2	0.812	0.733	0.097	211	134	432	96	6	0.742	5.54
Global 2018 Hatchery	**449**	**13.3**	**0.815**	**0.728**	**0.109**	**297**	**214**	**441**	**441**	**6**	**0.700**	**6.00**

Table 3. continued

Captive spawned	N	N_{AC}	H_{EC}	H_{OC}	F_{IS}	N_{eD}	-95	+95	N	N_h	*h*	H_R
18CSDX-001	197	14.2	0.790	0.701	0.107	334	201	787	196	7	0.711	4.60
ABP16_001_004	50	14.4	0.791	0.682	0.145	103	58.7	288	50	6	0.56	4.70
ABP18_1CS	49	13.4	0.782	0.701	0.101	573	120	∞	47	7	0.49	5.74
Global 2019 Hatchery	296	14.4	0.804	0.714	0.115	422	286	732	291	8	0.67	5.90
ABP19_CS	50	13.92	0.813	0.701	0.14	78	59	111	50	6	0.635	6.00
DX_YC19	147	13.4	0.796	0.615	0.22	1056	417	∞	147	6	0.727	5.52
Los Lunas released	101	13.87	0.816	0.737	0.1	62	55	72	101	6	0.704	5.78
Global 2020 Hatchery	298	14.58	0.812	0.676	0.17	220	175	286	298	7	0.716	5.02
2021_caplot_SNARRC	101	14.31	0.826	0.729	0.126	187	108	510	101	8	0.658	6.35
2021_4WIF1_LLSMR	100	14.15	0.806	0.72	0.109	108	72	188	99	7	0.702	6.88
2021_caplot_ABP	48	12.9	0.817	0.742	0.094	81	38	722	48	5	0.652	5.00
2021 Global Hatchery	249	14.57	0.821	0.728	0.118	269	286	443	248	9	0.685	7.68

Table 3. continued

Broodstock	N	N_{AC}	H_{EC}	H_{OC}	F_{IS}	N_{eD}	-95	95	N	N_h	*h*	H_R
2018 ABQ BioPark-Bs-YC17**	110	14.2	0.808	0.694	0.147	967	314	∞	110	5	0.659	4.73
2018 SNARRC- Bs-YC17**	59	12.7	0.819	0.692	0.158	617	169	∞	59	7	0.728	6.53
2018 ABQ BioPark-Bs-YC18**	123	14.9	0.82	0.729	0.117	385	209	1095	104	7	0.72	7.2
2018 SNARRC- Bs-YC18**	356	14.2	0.812	0.727	0.109	1551	370	∞	338	10	0.7	7.07
2019 ABQ BioPark- Bs 2019-YC16/17	191	14.6	0.810	0.689	0.148	2892	569	∞	191	8	0.672	5.96
2019 SNARRC- Bs 2019-YC17	176	12.9	0.790	0.700	0.110	191	222	372	175	8	0.705	5.04
2019 LLSMR- Bs 2019-YC18	186	14.5	0.810	0.719	0.118	449	222	3338	188	9	0.706	5.49
2020 ABQ BioPark-Bs-YC15	100	14	0.808	0.7	0.14	406	242	1083	101	5	0.499	4.71
2020 ABQ BioPark-Bs-YC18	99	14.4	0.799	0.719	0.10	615	306	10399	100	7	0.687	6.29
2020 SNARRC- Bs_YC17	99	15	0.827	0.744	0.100	160	124	217	99	8	0.665	6.68
2020 SNARRC- Bs_YC18	100	14.8	0.805	0.678	0.15	477	265	1832	100	8	0.709	7.37
2020 SNARRC- Bs_YC19	96	15.5	0.821	0.738	0.100	495	239	2047	97	9	0.649	7.13
2020 LLSMR-Bs-ABP18-4WI	138	15.6	0.833	0.731	0.112	∞	2285	∞	137	10	0.740	7.48
2021 ABQ BioPark-Bs-YC16	98	14.83	0.813	0.703	0.128	1289	276	∞	98	8	0.670	7.25
2021 ABQ BioPark-Bs-YC19	199	15.05	0.818	0.714	0.129	2225	686	∞	199	10	0.722	7.66
2021 ABQ BioPark-Bs-YC20	258	14.87	0.813	0.715	0.124	3255	722	∞	258	10	0.710	6.45
2021 SNARRC- Bs-YC20	199	15.02	0.810	0.705	0.131	∞	296	∞	198	10	0.725	6.83
2021 LLSMR-Bs-YC19	50	15.29	0.827	0.747	0.099	1072	383	∞	50	8	0.799	7.96
2021 LLSMR-Bs-YC20	149	14.64	0.806	0.723	0.104	3046	625	∞	148	9	0.706	7.28

Figure 1. Annual diversity metrics calculated from microsatellite loci. Estimates of gene diversity and heterozygosity obtained from resampling of microsatellites (H_{EC} and H_{OC}) and haplotype diversity (*h*) from mitochondrial data are shown in the upper panel, and number of alleles (N_{AC}) and haplotypes (H_R) are shown in the lower panel. Dashed (H_{EC} and N_{AC}) and dotted (H_{OC}) lines indicate diversity benchmarks obtained using a resampling procedure and correspond to a minimum sample size of n=43.

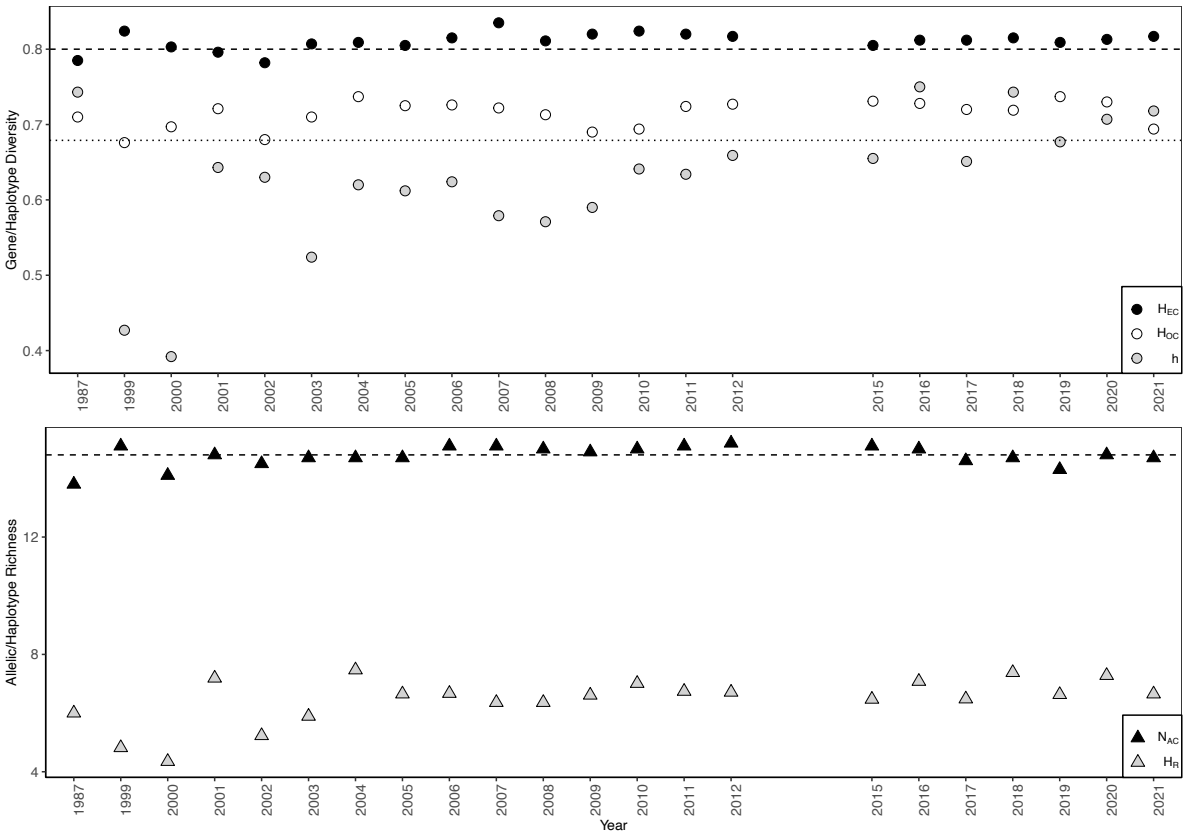

Figure 2. Annual diversity metrics of wild Rio Grande Silvery Minnow by reach (Angostura, Isleta, San Acacia). Microsatellites diversity estimates, gene diversity (top), heterozygosity (middle), allelic diversity (bottom) were corrected for differences in sample sizes across years by resampling.

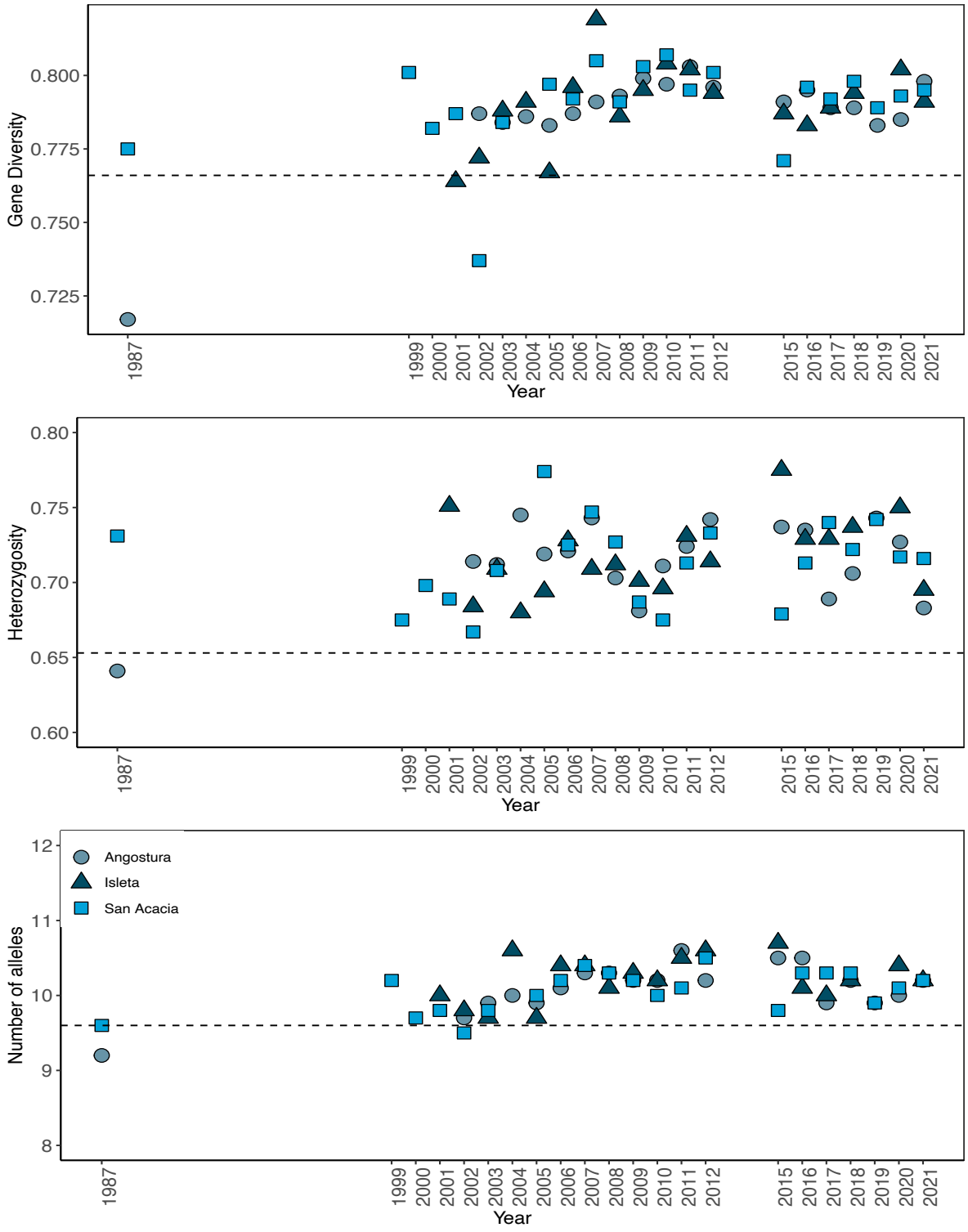

Figure 3. Annual mtDNA diversity metrics of wild Rio Grande Silvery Minnow by year and river reach. Estimates of mtDNA haplotype diversity are shown in the upper panel and haplotype richness are shown in the lower panel.

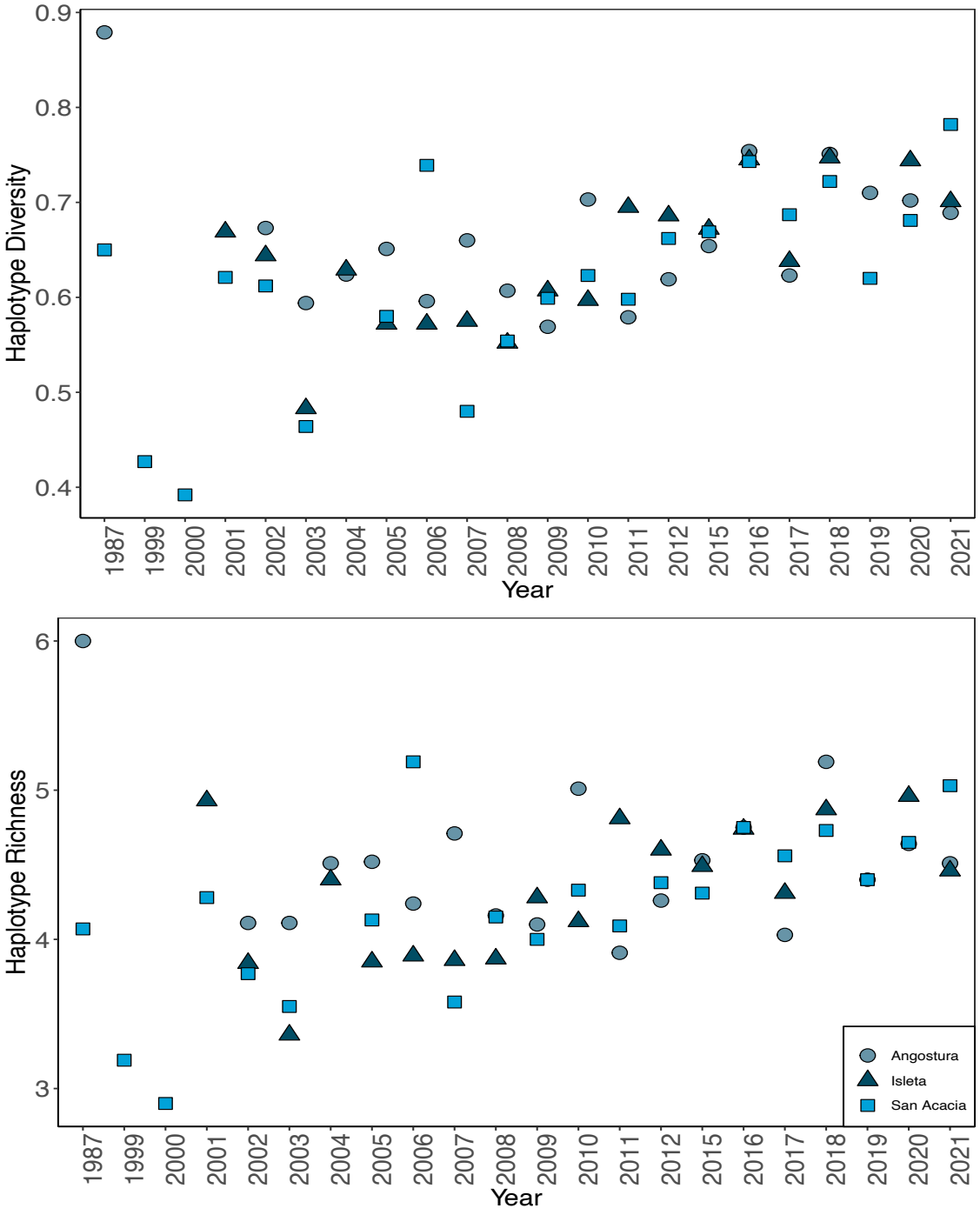

Genetic diversity statistics based on microsatellite data of 'wild' Rio Grande Silvery Minnow sampled in 2021 (H_{EC}= 0.817, H_{OC} = 0.694, and N_{AC}= 14.7) were within the range of values observed since monitoring began (Table 3, Fig. 1). The lowest number of alleles and heterozygosity were observed in the 1987 sample (N_{AC} = 13.8, H_{OC} = 0.676) and lowest gene diversity (H_{EC}= 0.782) was recorded in 2002; prior to the commencement of population augmentation. We used a resampling approach of all 'wild' fish collected between 1987-2021 to determine diversity benchmarks based on microsatellites that correspond to annual diversity estimates based on the minimum annual sample size (n = 43 [year], n=15 [reach]). Diversity benchmarks at the annual level were H_{EC} = 0.80, H_{OC} = 0.679, and N_{AC}= 14.8 and H_{EC} = 0.766, H_{OC}= 0.653, and N_{AC}= 9.6 at the reach level (Fig 1). Gene diversity and heterozygosity for 2021 'wild' fish exceeded these benchmarks. From analysis of microsatellite data by river reach all diversity metrics for the 2021 sample exceeded the minimum benchmark values.

Across all captive stocks genotyped in 2021, gene diversity, heterozygosity and allelic diversity for pooled captive lots released to the Rio Grande in fall 2020 were greater than the lower 95% CI genetic diversity benchmark (Table 3). Allelic diversity fell below the benchmark estimates while heterozygosity exceeded benchmark estimates in individual captive stocks released in fall 2020. All measures of genetic diversity in the refugial broodstocks sampled in 2020 from the three facilities, were very similar to estimates in the middle Rio Grande population (Table 3).

MtDNA- genetic diversity

A total of 17 mtDNA haplotypes have been identified from assaying 6464 wild (untagged) individuals from the middle Rio Grande from 1987 to 2021 (Table 4). Haplotype A was the most common in almost all samples including the 2021 collections. In the 2021 'wild' population, haplotype A was present in 46% of individuals, haplotypes (C, D, F, M) were present at moderate frequencies (6-21% of individuals) and three haplotypes (I, K, 0) were uncommon (<5%). For the first time since genetic monitoring commenced, haplotype E was not detected in the Middle Rio Grande population in 2021. At the reach level in 2021, seven to eight haplotypes were detected and mtDNA diversity statistics decreased over 2020 values (Figure 3). Haplotype diversity and haplotype richness were marginally higher in the San Acacia reach (h= 0.782, H_R= 5.03) compared to both the Angostura and Isleta reaches (h=0.69-0.70, H_R= 4.5) in 2021. Across the time series, haplotype diversity exceeded 0.7 in the 1987, 2016, 2018, 2020 and 2021 samples and was the lowest in 2000 (h = 0.392) (Table 3, Figure 3). In 2021, haplotype diversity ranged from 0.718 ('wild') to 0.67 (ABQ BioPark Bs YC16). Both haplotype diversity in 2021 'wild' samples increased over values in 2020 (Figure 3; Table 3) while haplotype richness was reduced. In 2021, three rare haplotypes (I, Q and V) were detected in a small number of hatchery individuals but these haplotypes were not seen in the 2021 wild sample. Eight to ten haplotypes were observed in the BioPark broodstocks, 10 haplotypes were observed in the Southwestern ARRC broodstocks and 8-9 haplotypes were detected in the LLSMR broodstocks (Table 5).

Population structure- microsatellites

In 2021, there were no significant differences between Rio Grande Silvery Minnow collected in the three river reaches (F_{ST}=0.0004 [-0.004 – 0.006] between Angostura and Isleta, F_{ST}=0.002 [-0.002 – 0.008] between Angostura and San Acacia, and F_{ST}=0.006 [-0.009 – 0.016] between Isleta and San Acacia) following Bonferroni correction. Across the time series (1999-2021), average values of pairwise F_{ST} were three times smaller (2015-2021 F_{ST}=0.002) for comparisons after the 2012-2014 population bottleneck

compared to comparisons preceding it (1999-2012; F_{ST}=0.006) (Figure 4). Total population structure was evaluated by considering global F_{ST} estimates across all 2021 samples, including hatchery stocks and broodstock (Figure 5). Samples from the middle Rio Grande collected in 2021 differed significantly from almost all captive stocks with values of F_{ST} ranging from 0.003 to 0.006. However, divergence was less than that seen between the wild 2020 sample. There were also significant allele frequency differences among most captive stocks.

Population structure- mtDNA

Total population structure was evaluated using Φ_{ST} estimates across all 2021 samples, including hatchery stocks and broodstock (Table 7) based on mtDNA haplotype frequencies. We also included the 2019 and 2020 sample collected from the middle Rio Grande population. After Bonferroni correction, there were no significant pairwise comparisons. Φ-statistics were also calculated from mtDNA data across all wild-caught Rio Grande Silvery Minnow across the time-series (1987, 1999-2021). Likewise, a significant proportion of variance was not explained by differences among groups (Φ_{CT}=0.04, p-value=0.297), or within groups (Φ_{SC}=0.0004, p-value=0.093) or among individual samples (Φ_{ST}=0.002, p-value=0.057).

Genetic differences among the Angostura, Isleta, and San Acacia reaches were not significant across the time series (Φ_{CT} = 0.0008, P = 0.136). Likewise, pairwise Φ_{ST} between reaches in 2021 were small and not significantly different from zero (Φ_{ST}=0.002, p-value=0.257 between Angostura and Isleta; Φ_{ST}=-0.002, p-value=0.420 between Angostura and San Acacia, Φ_{ST}= -0.005, p-value=0.537 between Isleta and San Acacia).

Genetic effective size

Temporal and MLNE estimates of variance effective size, N_{eV}, from microsatellites, are shown in Figure 6. For 2020-2021, estimates of N_{eV} across methods ranged from 53-240; a substantial decline from the previous time period (2019-2020). MLNE and temporal estimates of female variance effective size, N_{ef}, based on mtDNA are shown in Figure 7. For 2020-2021 temporal comparison, estimates of N_{ef} decreased from the previous time period to N_{ef}= 69 (95% CI 13-695) for the temporal method and N_{ef} = 56 (95% CI 30-311) calculated using the maximum likelihood method.

Inbreeding effective size (N_{eD}) was 1263 (95% CI 723-4219) for wild fish collected in 2021; a decline from the 2020 estimate (Figure 8; Table 2). For captive stocks released in the middle Rio Grande in fall 2020 from Albuquerque BioPark, N_{eD} was 81. Effective size of captive stocks from Southwestern ARRC was N_{eD} = 187 and from LLSMR N_{eD}=108.

Estimates of N_{eD} of refugial broodstock held at the Albuquerque BioPark ranged from N_{eD} = 1289 (YC16) and N_{eD} = 3255 (YC20), LLSMR ranged from 1072 (YC20) to infinite and for Southwestern ARRC N_{eD} = 3046 (YC20). These values reflect the effective size of the generation preceding the broodstock samples.

Figure 4. Pairwise F_{ST} among temporal collections (1987, 1999-2012, 2015-2021). 95% Confidence intervals are shown around point estimates.

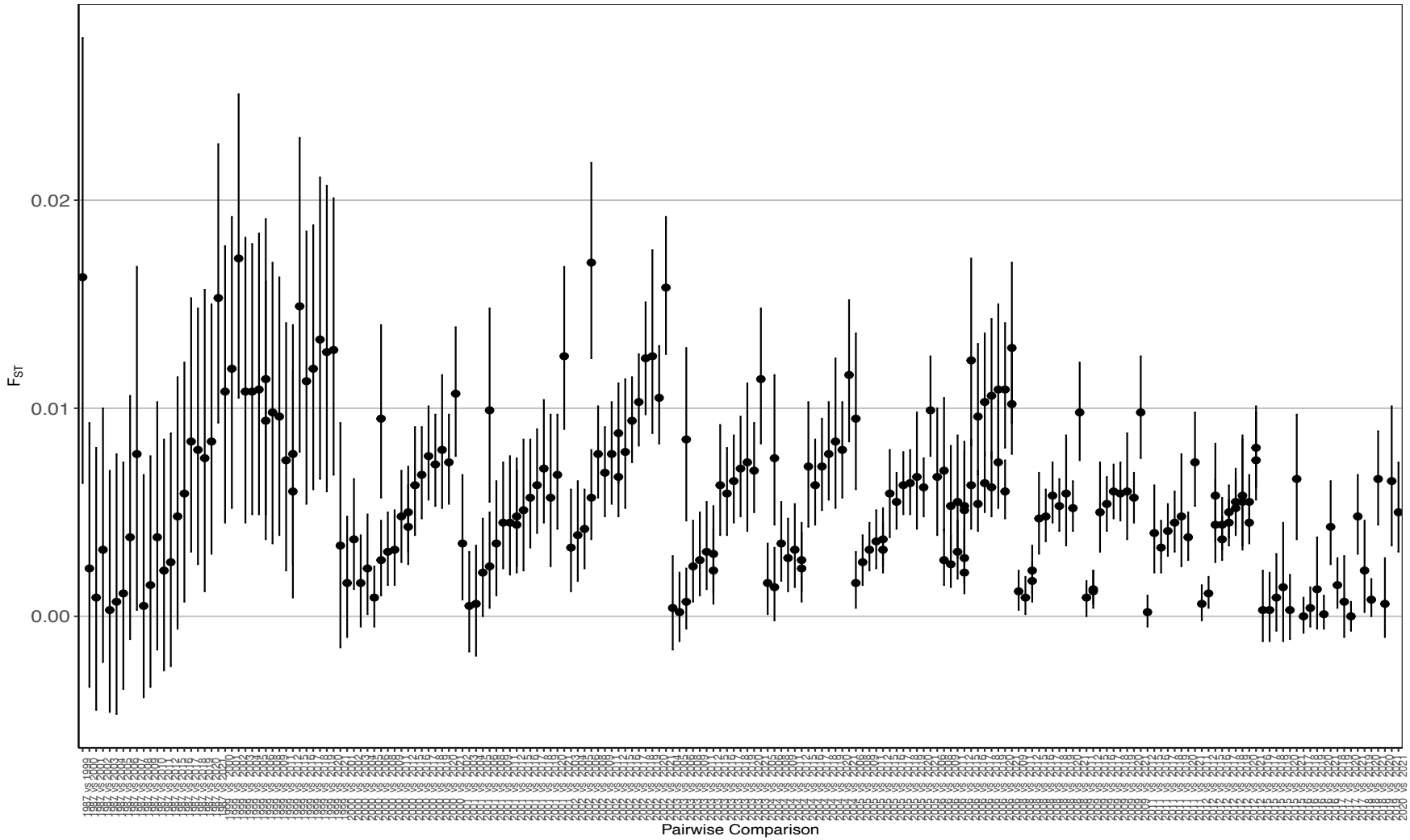

Figure 5. Pairwise F_{ST} values and associated p-values calculated based on microsatellites for 'wild' (2020 and 2021), captive stocks released in fall 2020, and refugial broodstocks (BS) held at Southwestern ARRC, Albuquerque Biopark and the LLSMR. Point estimates with 95% CIs that overlap with zero are not significant (i.e., allele frequencies are not different between samples).

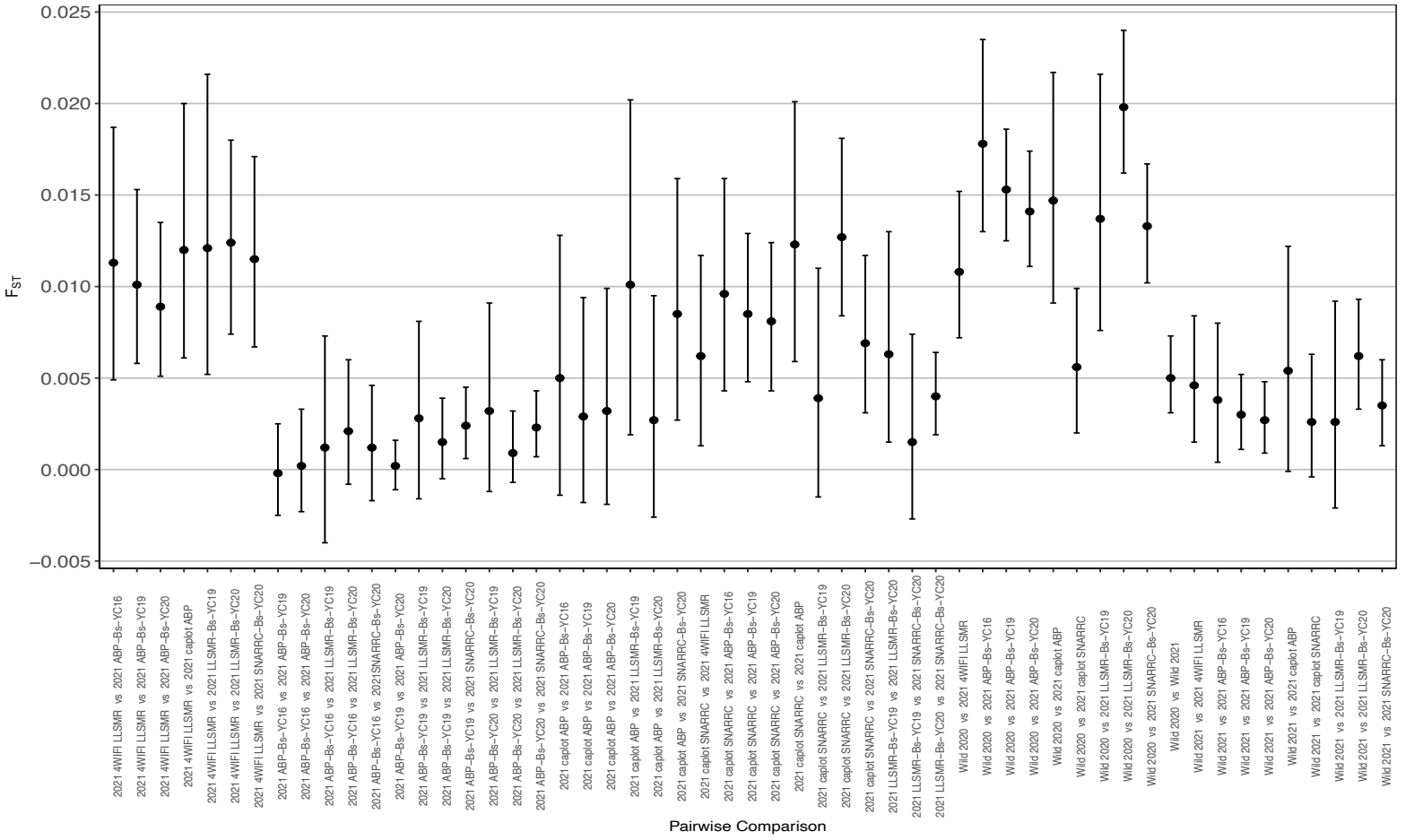

Figure 6. Variance effective size (N_{eV}) calculated from microsatellite data, as based on MLNE (upper), Nei and Tajima method (middle), and TEMPOFS (lower) estimates and their associates 95% CIs. TEMPOFS estimate from 2011-2012 (value not shown) was infinite. Upper error bars extending to y-maxima indicate infinite upper estimate bounded 95% CI.

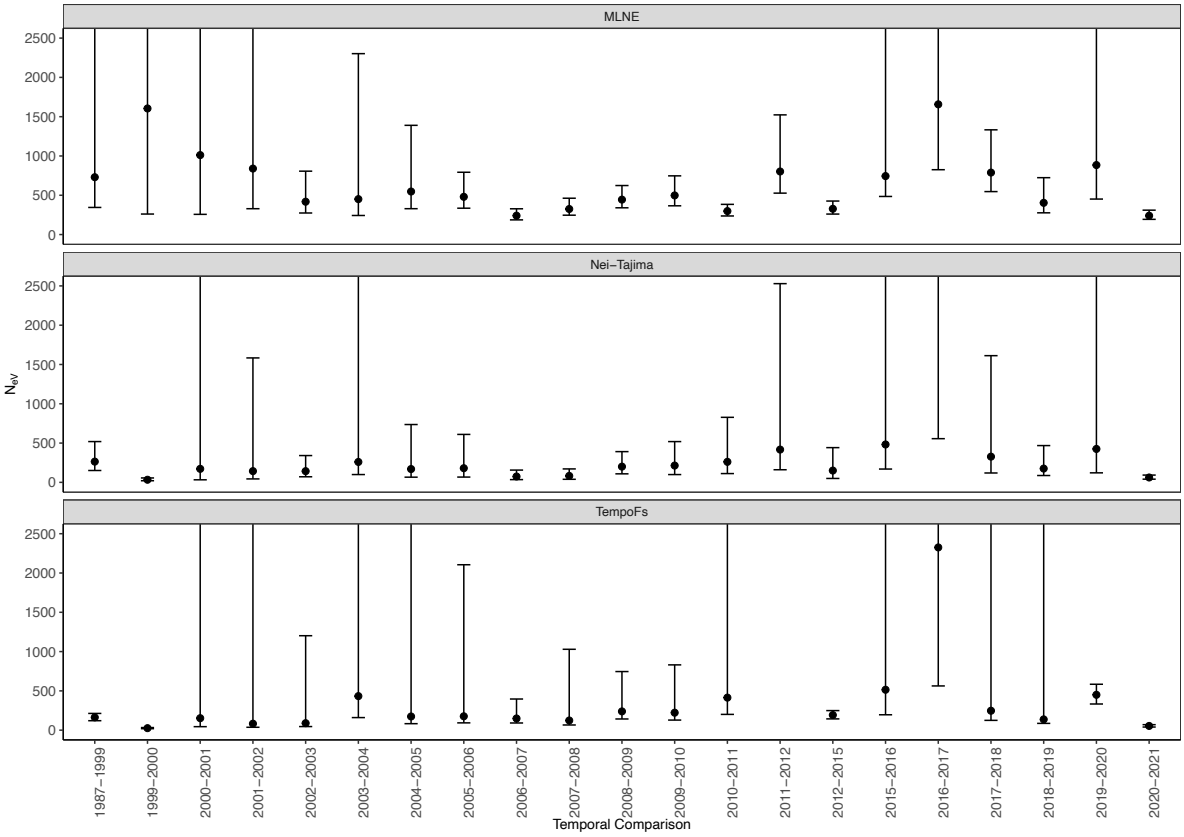

Figure 7. Female variance effective size estimates (N_{ef}) and their associated 95% CIs, based on mtDNA data and calculated using MLNE (upper) and temporal (moments) (lower) methods. Infinite mean estimates are indicated by points falling outside of the plot area and upper error bars extending to y-maxima indicate infinite upper bounded 95% CI.

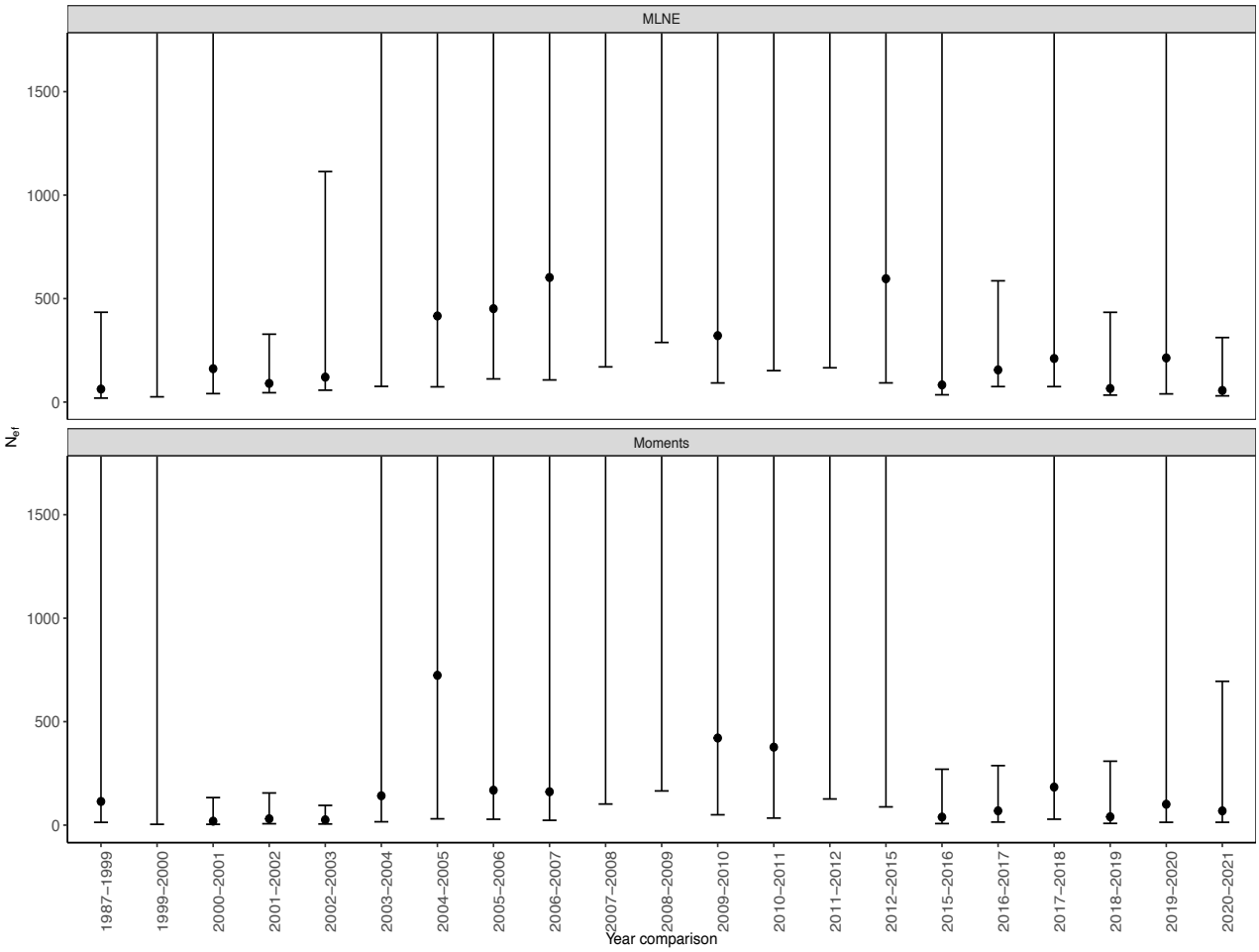

Figure 8. Estimates of inbreeding effective size (N_{eD}) and their associated 95% confidence intervals. Note the logarithmic scale on y-axis. Infinite mean estimates are indicated by points lying at y-maximum, and upper error bars extending to y-maximum indicate infinite upper bounded 95% CI.

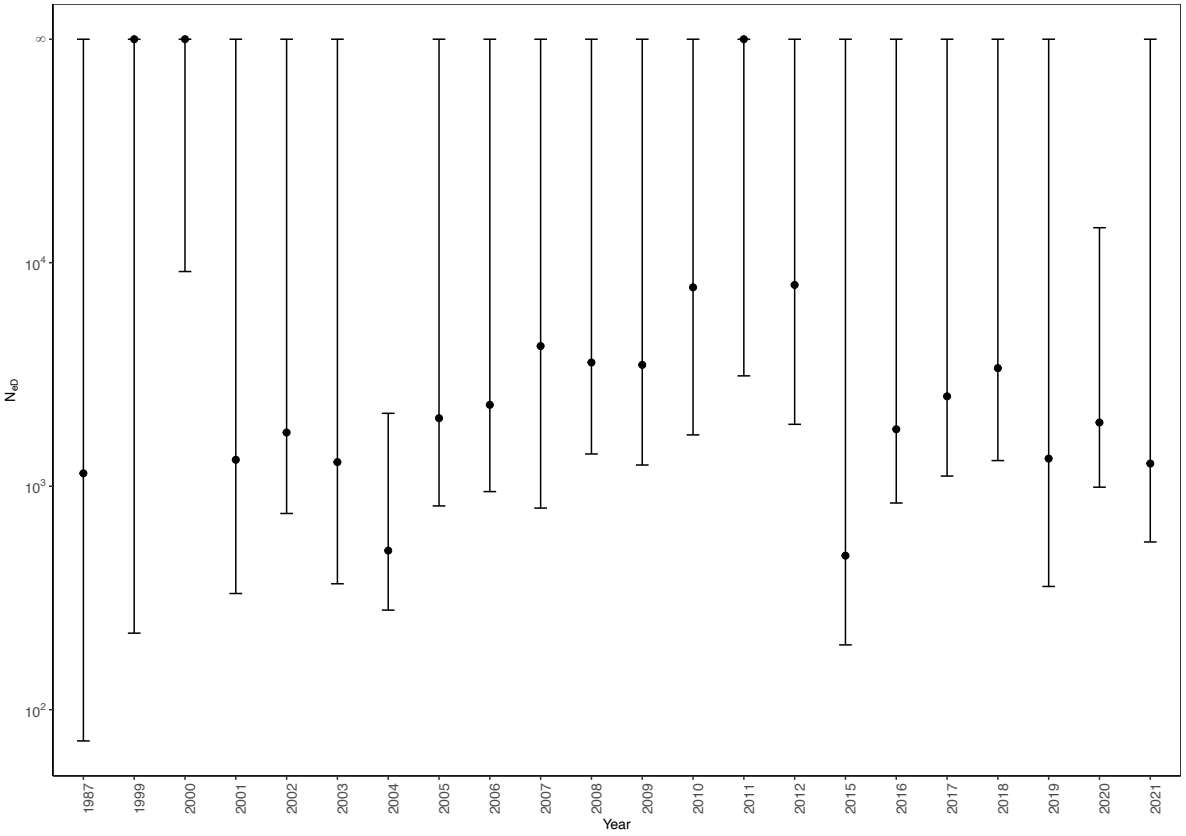

DISCUSSION

Genetic monitoring

Monitoring genetic diversity parameters (H_E, H_O, A_R and N_e) across contemporary time-series can illuminate demographic and evolutionary processes affecting wild and captive populations that are unattainable using standard demographic sampling approaches. To our knowledge, data from Rio Grande Silvery Minnow is one of the longest genetic monitoring time-series for any non-salmonid freshwater fish; spanning 34 years comprising 23 temporal samples (1987, 1999-2012, 2015-2021). Annual monitoring of the genetic status of both 'wild' Rio Grande Silvery Minnow in the middle Rio Grande in addition to representative captive stocks repatriated to the river allows assessment of whether management actions are maintaining levels of genetic diversity in the species. Maintenance of diversity is critical because genetic diversity facilitates adaptation and responses to changing conditions.

Status of the 'wild' (i.e. untagged) Rio Grande Silvery Minnow population in 2021

The population monitoring program for Rio Grande Silvery Minnow (1993-2021) shows that the wild population has experienced multiple, order-of-magnitude changes in density over the past two decades (Dudley et al. 2021). The period from 2015-2017 saw abundances of Rio Grande Silvery Minnow increase substantially over values recorded between 2012-2014; demonstrating the capacity of the species to rebound

rapidly following periods of very low density. Subsequently, there was a 99.6 % decline in estimated density between 2017 and 2018 (Dudley et al. 2018) associated with extensive channel drying (> 60 km) between April through October 2018 and almost complete recruitment failure (Archdeacon et al. 2020a). This occurred as a result of a period of moderate to severe drought that extended from December 2017 to February 2019 (Archdeacon et al. 2020a). In 2019, the population increased 2,285% over densities seen in the previous year associated with extended high spring flows and minimal channel drying and strong recruitment (Dudley et al. 2020; Archdeacon et al. 2020a). However, 2020 brought another substantial decline (-88.8%) in the population (Dudley et al. 2021). Repeated changes in population size, particularly repeated bottlenecks, are expected to gradually erode genetic diversity in the absence of actions to buffer the population (i.e. supportive breeding and augmentation). From 1987 and 1999-2004, both microsatellites and mtDNA showed considerable inter-annual variability in gene diversity metrics and effective size estimates. Following commencement of population supplementation with fish reared in captivity, inter-annual variability in diversity measures decreased from 2005 to 2012 and during this period there were marginal increases in mtDNA and microsatellite diversity. From 2006 to 2012 and 2015-2016 allelic diversity remained above the benchmark for this metric. More recently (2017-2021) this diversity measure has been at or below the benchmark. These results demonstrate that although the augmentation program has been critical in maintaining diversity in the face of repeated population bottlenecks, results for 2021 emphasize the importance of maintaining large and diverse captive stocks.

Genetic effective size

Genetic effective population size (N_e) is a key parameter in genetic monitoring programs because N_e determines the amount of variation that is transmitted to the next and at smaller N_e, diversity is lost more rapidly. Genetic effective population size estimates based on changes in allele frequencies from one year to the next revealed a substantial decline in 2021 with N_{eV} and N_{ef} estimates among the lowest (<100) since genetic monitoring began. The decrease in N_{eV} reflects strong genetic drift in allele frequencies between the breeding populations in 2020 and 2021. Estimates of female effective size made from mtDNA haplotype frequency data were consistent with the microsatellite data demonstrating reduced maternal contributions compared to the previous time period; consistent with the substantial decline in density identified by population monitoring of Rio Grande Silvery Minnow in 2020 compared to 2019 (Dudley et al. 2021).

Linkage disequilibrium effective size (N_{eD}=1263) also decreased from values in 2020 (N_{eD}=1927). It is important to note that N_{eD} estimates reflect the effective size of the parental generation of the sample. Hence, the higher effective size reported in 2020 reflects the size of the breeding population in 2019. It is important to note that ~200,000 fish were used in augmentation efforts in fall 2018, presumably some of these fish contributed to the substantial population increase associated with extended high spring flows and minimal channel drying and strong recruitment in 2019 (Dudley et al. 2020; Archdeacon et al. 2020a). Linkage disequilibrium is a single sample estimator and uses different aspects of the data to estimate the effective size. From a management perspective, there are a number of theoretical and practical distinctions between N_{eI} (inbreeding effective size, to which N_{eD} estimates are most closely associated) and N_{eV} (variance effective size). These two measures of effective size should be similar in stable populations but show predictable differences in declining (or growing) populations. For example, in declining populations N_{eI} should be larger than N_{eV} because the latter depends on the amount of genetic drift between sampled generations but the former is a measure of inbreeding in the generation prior to sampling, (Allendorf & Luikart 2007); therefore, N_{eI} is only reduced once mating between close relatives becomes more common

(i.e., homozygosity increases in the population). In previous years, we observed a disparity between N_{eD} and N_{eV} and this trend continued in 2020. Carson et al. (2020) investigated the relationship between N_{eD} and N_{eV} using simulations and showed that the disparity between N_{eV} and N_{eD} is driven by the interaction of population augmentation and fragmentation. Specifically, when upstream dispersal is disrupted by barriers (e.g., dams) N_{eI} is negatively associated with the rate of downstream dispersal (i.e., N_{eI} declines with higher rates of downstream movement) while N_{eI} is positively associated with supplementation rate (i.e., N_{eI} increases with higher rates of supplementation). In contrast, N_{eV}, is negatively associated with both bidirectional dispersal rates and supplementation relative to equilibrium N_e.

Genetic diversity of captive stocks released to the middle Rio Grande, New Mexico

In fall 2020, 218,500 fish were released in the middle Rio Grande, New Mexico. Gene diversity and heterozygosity for pooled captive lots released to the Rio Grande in fall 2020 were greater than the lower 95% CI genetic diversity benchmark. Allelic diversity fell below the benchmark estimates while heterozygosity exceeded benchmark estimates in individual captive stocks released in fall 2020. In 2021, mitochondrial haplotype richness (corrected for differences in sample size) was fairly consistent among captive lots and facilities. Preservation of genetic diversity in captive lots is critical because these fish periodically reestablish the species in the middle Rio Grande (e.g., 2014 and 2018).

Genetic Analysis of Broodstock

In 2021, we genotyped fish representing the 2016, 2019, and 2020 broodstock year classes. All measures of genetic diversity in these stocks were very similar to estimates in the middle Rio Grande population. However as in previous years, haplotype representation and frequencies of rare haplotypes differed between lots and facilities, such that not all haplotypes were identified in all refugial populations. This result highlights the continued need to maintain multiple refugial populations across different facilities and the importance of spawning large numbers of individuals to preserve rare alleles.

CONCLUSIONS

More than two decades of genetic monitoring of the 'wild' middle Rio Grande population and of released captive reared/bred Rio Grande Silvery Minnow provides a rare opportunity to track the genetic effects of population fluctuations associated with inter-annual variability in flows and of key management activities. The results presented here indicate that the trajectory of genetic change in the wild Rio Grande Silvery Minnow population is now determined largely by supplementation with captive reared stocks. Supplementation buffers the population against potential losses of diversity predicted by drastic changes in population size (Osborne et al. 2012). Levels of genetic diversity including heterozygosity and average number of alleles have so far been maintained over the duration of the study, with these key metrics all above the benchmarks. This highlights the importance of continued monitoring of both released captive stocks, broodstocks and the middle Rio Grande population as any detrimental effects (such as losses of diversity) in the captive stocks will ultimately be transferred to the 'wild' population.

ACKNOWLEDGEMENTS

We gratefully acknowledge the assistance of David Camak, Alexander Cameron, Gregor Hamilton, Huachan Liang, Samuel McKitrick and Melissa Sanchez (UNM Molecular Biology Core Facility), Emily DeArmon,

and curatorial assistants (UNM Museum of Southwestern Biology, Division of Fishes), Manuel Ulibarri and Wade Wilson (USFWS) and Thomas Archdeacon (USFWS), Kathy Lang and Kim Ward (Albuquerque Biological Park), Alison Hutson (Los Lunas Silvery Minnow Refugium) and Jennifer Bachus, Eric Gonzales and Joel Lusk (Bureau of Reclamation).

LITERATURE CITED

Allendorf, F.W., and G. Luikart. 2007. Conservation and the genetics of populations. Blackwell Publishing, Malden, MA, USA.

Archdeacon, T.P. and J.K. Reale. 2020a. No quarter: Lack of refuge during flow intermittency results in catastrophic mortality of an imperiled minnow. *Freshwater Biology*, Early view, https://doi.org/10.1111/fwb.13607

Archdeacon, T. P., Diver-Franssen, T. A., Bertrand, N. G., and Grant, J. D. 2020b. Drought results in recruitment failure of Rio Grande silvery minnow (*Hybognathus amarus*), an imperiled, pelagic broadcast-spawning minnow. *Environmental Biology of Fishes*, 103, 1033–1044.

Bessert, M. L., and G. Ortí. 2003. Microsatellite loci for paternity analysis in the fathead minnow, *Pimephales promelas* (Teleostei: Cyprinidae). *Molecular Ecology Notes,* 3, 532-534.

Bestgen, K. R., and S. P. Platania. 1991. Status and conservation of the Rio Grande Silvery Minnow, *Hybognathus amarus*. *Southwestern Naturalist*, 36, 225-232.

Carson, E.W., Osborne, M.J. and T.F. Turner. 2020. Relationship of effective size to hatchery supplementation and habitat connectivity in a simulated population of Rio Grande Silvery Minnow. *North American Journal of Fisheries Management*, 40(4), 922-938.

Cook, J. A., K. R. Bestgen, D. L. Propst, and T. L. Yates. 1992. Allozymic divergence and systematics of the Rio Grande Silvery Minnow, *Hybognathus amarus* (Teleostei: Cyprinidae). *Copeia*, 1998, 6-44.

Dimsoski, P., G. Toth, and M. Bagley. 2000. Microsatellite characterization in central stoneroller *Campostoma anomalum* (Pisces: Cyprinidae). *Molecular Ecology*, 9, 2187-2189.

Do, C., R. S. Waples, D. Peel, G. M. Macbeth, B. J. Tillett, and J. R. Ovenden. 2014. NeEstimator V2: re-implementation of software for the estimation of contemporary effective population size (N_e) from genetic data. *Molecular Ecology Resources*, 14, 209-214.

Dowling, T. E., Minckley, W. L., Marsh, P. C., and E. S. Goldstein. 1996. Mitochondrial DNA variability in the endangered razorback sucker (*Xyrauchen texanus*): analysis of hatchery stocks and implications for captive propagation. *Conservation Biology*, 10, 120-127.

Dudley, R. K., S. P. Platania, and G. C. White. 2014. Rio Grande Silvery Minnow Population Monitoring Program results from May to December. Report submitted to the U.S. Bureau of Reclamation Albuquerque Office. 151 pp.

Dudley, R. K., S. P. Platania, and G. C. White. 2018. Rio Grande Silvery Minnow Population Monitoring Program during September 2018. Report submitted to the U.S. Bureau of Reclamation Albuquerque Office. 35 pp.

Dudley, R. K., S. P. Platania, and G. C. White. 2021. Rio Grande Silvery Minnow Population Monitoring Program during 2020. Report submitted to the U.S. Bureau of Reclamation Albuquerque Office. 179 pp. 10.13140/RG.2.2.14448.79360

Excoffier, L., G. Laval and S. Schneider. 2005. Arlequin ver. 3.0: An integrated software package for population genetics data analysis. *Evolutionary Bioinformatics Online*, 1, 47-50.

Frankham, R. 2005. Genetics and extinction. *Biological Conservation*, 126, 131-140.

Goudet, J., and T. Jombart. 2020. *hierfstat:* Estimation and tests of hierarchical F-statistics.

Guo, S. W. and E. A. Thompson. 1992. Performing the exact test of Hardy–Weinberg proportion for multiple alleles. *Biometrics*, 48, 361-372

Hedrick, P. W. 1999. Perspective: Highly variable genetic loci and their interpretation in evolution and conservation. *Evolution*, 53, 313-318.

Hill, W. 1981. Estimation of effective population size from data on linkage disequilibrium. *Genetical Research*, 38, 209-216.

Hillis, D., C. Mable and B. Mable. 1996. Molecular Systematics. Sinauer Associates, Sunderland, MA, USA.

Horwitz, R.J., Keller, D.H., Overbeck, P.F., Platania, S.P., Dudley, R.K. and E.W. Carson. 2018. Age and Growth of the Rio Grande Silvery Minnow, an Endangered, Short-Lived Cyprinid of the North American Southwest. *Transactions of the American Fisheries Society*, *147*(2), 265-277.

Goudet, J., and T. Jombart. 2015. hierfstat: Estimation and tests of hierarchical F-Statistics. R package version 0.04-22. Retrieved from https://CRAN.R-project.org/package=hierfstat

Jorde, P. E., and N. Ryman. 1995. Temporal allele frequency change and estimation of effective in populations with overlapping generations. *Genetics*, 139, 1077-1090.

Jorde, P. E., and N. Ryman. 1996. Demographic genetics of brown trout (*Salmo trutta*) and estimation of effective population size from temporal change of allele frequencies. *Genetics*, 143, 1369-1381.

Jorde, P. E., and N. Ryman. 2007. Unbiased estimator for genetic drift and effective population size. *Genetics*, 177, 927-935.

Keenan, K., McGinnity, P., Cross, T.F., Crozier, W.W. and P.A. Prodöhl. 2013. diveRsity: An R package for the estimation and exploration of population genetics parameters and their associated errors. *Methods in ecology and evolution*, 4(8), 782-788.

Laurie-Ahlberg, C. C., and B. S. Weir. 1979. Allozyme variation and linkage disequilibrium in some laboratory populations of *Drosophila melanogaster*. *Genetics*, 92, 1295-1314.

Nei, M., 1987. *Molecular evolutionary genetics*. Columbia university press.

Nei, M., and F. Tajima. 1981. Genetic drift and estimation of effective population size. *Genetics*, 98, 625-640.

Osborne, M. J., S. R. Davenport, C. R. Hoagstrom, and T. F. Turner. 2010. Genetic effective size, N_e, tracks density in a small freshwater cyprinid, Pecos bluntnose shiner (*Notropis simus pecosensis*). *Molecular Ecology*, 19, 2832-2844.

Osborne, M. J., E. W. Carson, and T. F. Turner. 2012. Genetic monitoring and complex population dynamics: insights from a 12-year study of the Rio Grande Silvery Minnow. *Evolutionary Applications*, 5, 553-574.

Osborne, M. J., and T. F. Turner. 2012. Genetic monitoring of the Rio Grande Silvery Minnow: genetic status of wild and captive stocks in 2012. 2012 Annual Report submitted to U. S. Bureau of Reclamation, Albuquerque Area Office. pp. 29.

Petit, R. J., A. El Mousadik, and O. Pon. 1998. Identifying populations for conservation on the basis of genetic markers. *Conservation Biology*, 12, 844-855.

Pflieger, W. L.1980. *Hybognathus nuchalis* Agassiz, Central silvery minnow. In D. S. Lee, C. R. Gilbert, C. H. Hocutt, R. E. Jenkins, D. E. McAllister, and J. R. Stauffer Jr., eds. *Atlas of North American Freshwater Fishes*, p. 177. North Carolina State Museum of Natural History, Raleigh, NC. Rousset, F., 2008. genepop'007: a complete re-implementation of the genepop software for Windows and Linux. *Molecular ecology resources*, *8*(1), pp.103-106.

Rice, W. R. 1989. Analyzing tables of statistical tests. *Evolution*, 43, 223-225.

Turner, T. F., L. A. Salter and J. R. Gold. 2001. Temporal-method estimates of N_e from highly polymorphic loci. *Conservation Genetics*, 2, 297-308.

Turner, T. F., T. E. Dowling, R. E. Broughton, and J. R. Gold. 2004. Variable microsatellite markers amplify across divergent lineages of cyprinid fishes (subfamily Leusicinae). *Conservation Genetics*, 5, 273-281.

Turner, T. F., M. J. Osborne, G. R. Moyer, M. A. Benavides and D. Alò. 2006. Life history and environmental variation interact to determine effective population to census size ratio. *Proceedings of the Royal Society London B*, 273, 3065-3073.

Schwartz, M. K., G. Luikart, and R. S. Waples. 2007. Genetic monitoring as a promising tool for conservation and management. *Trends in Ecology and Evolution*, 22, 11-16.

U.S. Fish and Wildlife Service., 1994. Endangered and threatened wildlife and plants: final rule to list the Rio Grande silvery minnow as an endangered species. *Federal Register*, 59, 36988–36995.

U. S. Fish and Wildlife Service., 2010. Rio Grande Silvery Minnow (*Hybognathus amarus*) recovery plan, first revision: Albuquerque, New Mexico.

U. S. Fish and Wildlife Service., 2018 Rio Grande Silvery Minnow genetics and propagation management plan, 2018 revision: Albuquerque, New Mexico.

Van Oosterhout, C., W. F. Hutchinson, D. P. M. Wills, and P. Shipley. 2004. MICRO-CHECKER: software for identifying and correcting genotyping errors in microsatellite data. *Molecular Ecology Notes*, 4, 535-538.

Wang, J. L. 2001. A pseudo-likelihood method for estimating effective population size from temporally spaced samples. *Genetical Research*, 78, 243-257.

Wang, J. and M. C. Whitlock, 2003. Estimating effective population size and migration rates from genetic samples over space and time. *Genetics*, 163, 429–446.

Waples, R. S. 1989. A generalized approach for estimating effective population size from temporal changes in allele frequency. *Genetics*, 121, 379-391.

Waples, R. S. 2005. Genetic estimates of contemporary effective population size: to what time periods do the estimates apply? *Molecular Ecology*, 14, 3335-3352.

Waples, R. S., and M. Yokota. 2007. Temporal estimates of effective population size in species with overlapping generations. *Genetics*, 175, 219-233.

Waples, R. S., and C. Do. 2010. Linkage disequilibrium estimates of contemporary N_{eV} using highly variable genetic markers: A largely untapped resource for applied conservation and evolution. Ev*olutionary Applications*, 3, 244-262.

Weir, B. S., and C. C. Cockerham. 1984. Estimating F-statistics for the analysis of population structure. *Evolution*, 38, 1358-1370.

Wright, S. 1931. Evolution in Mendelian populations. *Genetics*, 16, 97-159.

GLOSSARY

Allelic/ haplotype richness – The total number of alleles/haplotypes in a population corrected by rarefaction to account for differences in sample size among collections.

Genetic drift – is the random change in allele frequencies from generation to generation because of sampling error. Specifically, the finite number of genes passed on to progeny will be an imperfect sample of

the parental allele frequencies. The effects of genetic drift are (i) allele frequencies will change and (ii) genetic variation will be lost. The smaller the population, the greater the change in allele frequencies due to drift.

Genetic effective size (N_e) – The effective size of a breeding population under idealized conditions meeting the assumptions of Hardy-Weinberg (i.e., equal sex ratio, random mating).

Haplotype/ gene diversity (*h*) – Computationally equivalent to expected heterozygosity (H_e) but referred to as gene/haplotype diversity as there are no heterozygotes because mtDNA is haploid.

Hardy-Weinberg equilibrium – The stable frequency distribution of genotypes (AA, Aa, and aa) in the proportions (p^2, 2pq, and q^2) respectively (where p and q are the frequencies of the alleles, A and a). The Hardy-Weinberg principle makes the following assumptions (i) random mating (i.e. there is neither preference or aversion), (ii) no mutation (i.e. genetic information is transmitted from parent to progeny without change), (iii) large or infinite population size, (iv) no natural selection, (v) no immigration.

Heterozygosity (H_e) – The presence of different alleles at one or more loci on homologous chromosomes. Proportion of heterozygous individuals for a locus in a population.

Inbreeding co-efficient (F) – the probability that two alleles at a locus in an individual are identical by descent. Used to measure the extent of inbreeding.

Linkage disequilibrium – statistical association of alleles at different loci. Such association indicates that two loci are physically adjacent on a chromosome such that there is little recombination during meiosis.

Locus/Loci – A segment of DNA on a chromosome. Loci is the plural form of the noun.

Microsatellite – short tandem repeated DNA sequences e.g. ACACACAC. These loci usually have variable numbers of repeats within/among individuals and high heterozygosity.

Mitochondrial (mt) DNA – maternally inherited circular DNA molecule contained within the mitochondria.

Null allele – a mutation that occurs in a PCR primer site that prevents amplification during polymerase chain reaction (PCR).

Primers – short fragments of DNA that flank the DNA region of interest and which are used in PCR to target specific nuclear and mtDNA loci.

Polymerase chain reaction – method used to make copies through amplification of a specific segment of DNA (such as a microsatellite locus or mitochondrial DNA gene). DNA is heated in the presence of PCR primers, and the Taq polymerase enzyme, to copy the intervening DNA sequencing using ~30 cycles.

Ryman-Laikre effect – an increase in inbreeding and reduction in the total effective population size that can occur in wild-captive systems that occurs when few individuals contribute large numbers of offspring.

Wahlund effect – is a reduction in heterozygosity compared to Hardy-Weinberg expectations, and occurs in a population divided into partially isolated subpopulations

'Wild' vs. 'captive' – we use the term 'wild' to refer to unmarked fish sampled directly from the Rio Grande. 'Wild' fish may have parents that were wild or bred/reared in captivity, but were hatched in the Rio Grande. The term 'captive' refers to a fish held in a hatchery or a VIE-tagged fish captured from the Rio Grande.

Table 4. MtDNA haplotype frequencies for the wild middle Rio Grande population and fish reared from captive spawning. Values from 2021 monitoring year are shaded for emphasis.

	A	C	D	E	F	I	J	K	M	O	P	Q	S	T	V
1987	45.95	16.22	16.22	5.41	8.11	-	-	2.70	5.41	-	-	-	-	-	-
1999	75.00	-	11.36	6.82	4.55	-	-	2.27	-	-	-	-	-	-	-
2000	76.98	0.79	4.76	4.76	11.90	-	-	0.79	-	-	-	-	-	-	-
2001	57.43	10.89	4.95	3.96	9.90	0.99	0.99	8.91	0.99	0.99	-	-	-	-	-
2002	55.56	19.90	13.70	1.03	5.94	-	0.26	3.36	-	0.26	-	-	-	-	-
2003	67.07	5.39	14.97	2.99	5.39	-	0.60	1.20	0.60	1.80	-	-	-	-	-
2004	59.63	8.70	10.56	1.86	7.45	1.24	-	4.97	1.86	3.11	0.62	-	-	-	-
2005	59.69	12.76	8.93	2.81	8.42	1.53	0.26	1.79	2.81	1.02	-	-	-	-	-
2006	58.58	13.72	9.23	4.75	4.75	0.26	-	4.75	2.90	0.79	-	-	-	0.26	-
2007	62.84	11.01	8.26	2.29	8.72	0.46	-	3.67	0.46	1.83	-	0.46	-	-	-
2008	63.46	11.97	7.91	2.56	6.62	0.64	-	4.49	0.85	0.64	0.21	-	0.64	-	-
2009	61.57	14.01	7.64	2.76	6.37	0.64	0.42	3.40	1.70	1.06	0.21	-	0.21	-	-
2010	57.11	12.09	9.72	3.08	7.11	1.42	-	5.45	1.66	2.37	-	-	-	-	-
2011	57.38	14.21	10.86	2.79	6.41	0.56	-	3.06	3.06	1.11	-	0.28	0.28	-	-
2012	54.28	17.32	9.53	3.70	7.59	0.39	0.39	2.92	2.14	1.75	-	-	-	-	-
2015	55.24	12.59	12.59	1.40	9.79	-	-	2.10	2.10	4.20	-	-	-	-	-
2016	40.51	25.32	9.37	1.77	7.09	0.76	-	3.04	3.29	8.86	-	-	-	-	-
2017	55.44	14.93	10.66	1.28	7.04	0.21	-	1.92	2.13	6.18	-	-	-	-	0.21
2018	44.74	16.51	11.72	1.44	9.09	0.72	-	4.07	2.87	7.89	-	-	-	-	0.96
2019	50.76	23.48	3.79	3.03	4.55	-	-	3.03	1.52	9.85	-	-	-	-	-
2020	48.70	19.62	8.27	1.42	7.33	1.65	-	3.55	1.65	6.86	-	-	-	-	0.95
2021	46.25	21.25	12.50	-	5.83	1.25	-	2.08	6.25	4.58	-	-	-	-	-

Table 4 (cont.). MtDNA haplotype frequencies for the wild middle Rio Grande population and fish reared from captive spawning. Values from 2021 monitoring year are shaded for emphasis. Haplotypes P, Q, T are omitted from this tables of frequencies for captive stocks as they have not been detected in them.

Captive spawned	A	C	D	E	F	I	J	K	M	O	S	V
ABP13-003-04 WC	40.0	24.0	12.0	-	16.0	-	-	-	-	8.0	-	-
ABP16-003 CS	64.0	25.6	2.6	5.1	-	-	-	-	2.6	-	-	-
Uvalde 2016	38.0	21.0	23.0	-	-	-	-	-	-	14	-	-
16CSDX-003	37.0	22.2	14.1	3	17.1	-	-	1.0	-	5.1	-	-
16CSDX-004	37.8	35.7	5.1	-	-	-	-	6.1	-	14.3	1.0	-
16CSDX-005	39.0	28	24.0	-	5.0	3	-	-	-	1.0	-	-
ABP18	55.3	40.4	4.3	-	-	-	-	-	-	-	-	-
17CSDX_001	40.8	25.5	24.5	-	2.0	-	-	-	-	7.1	-	-
17CSDX_002	52.0	17.3	17.2	-	10.2	-	-	-	-	3.1	-	-
17CSDX_003	41.2	18.6	29.1	2	2.9	-	-	-	-	5.9	-	-
17CSDX_004	39.6	20.8	20.2	1	12.5	-	-	-	-	5.2	-	-
18CSDX_001	44.9	20.4	19.9	1.5	4.1	-	-	0.5	-	8.7	-	-
ABP18_CS	67.3	10.2	0.2	0.2	0.2	-	-	-	4.1	8.0	-	-
ABP16_001_004	60.0	24	2.0	-	8.0	-	-	-	4	2.0	-	-
ABP19_CS	57.1	18.4	6.1	-	2.0	-	-	8.2	-	8.2	-	-
DX_YC19	43.2	15.8	17.8	-	2.7	-	-	-	2.1	18.5	-	-
Los Lunas released	42.0	14.0	32.0	-	4.0	-	-	-	3.0	5.0	-	-
2021_caplot_SNARRC	53.5	18.8	14.9	-	5.0	1.0	-	1.0	1.0	5.0	-	-
2021_4WIF1_LLSMR	50.5	14.1	7.1	-	4.0	-	6.1	-	13.1	-	-	5.05
2021_caplot_ABP	43.8	39.6	4.2	-	10.4	-	-	-	-	2.1	-	-

Table 5. MtDNA haplotype frequencies for broodstock held at ABQ BioPark, Southwestern ARRC and the LLSMR. Samples collected for the 2021 monitoring year are shaded for emphasis. Haplotypes P, S, T are omitted from this table of frequencies for captive stocks as they have not been detected in them.

Broodstock	A	C	D	E	F	I	K	M	O	Q	V
ABQ Biopark-Bs-2017	50.0	26.3	10.9	-	2.7	-	-	-	9.1	-	-
SNARRC- Bs-2017	44.1	22	15.2	3.4	5.1	-	-	-	6.8	-	-
ABQ Biopark-Bs-2018	47.1	26	6.7	0.96	6.7	-	-	3.9	8.7	-	-
SNARRC- Bs-2018	49.4	17.1	13.6	1.2	6.8	1.5	0.9	0.6	8.3	-	0.6
ABQ Biopark-Bs-2019	53	14.2	15.3	-	4.9	0.6	3.3	3.3	5.5	-	-
SNARRC- Bs-2019	47.6	17.1	18.2	1.1	4.8	-	2.7	0.5	7.5	-	0.5
Los Lunas- Bs-2019	47.9	14.8	13.6	-	3.6	0.6	2.4	0.6	16.6	-	-
ABQ Biopark-Bs-2015	68.1	19.2	6.4	-	2.1	-	-	-	4.3	-	-
ABQ Biopark-Bs-2018	43.4	34.3	8.1	3.0	6.1	-	-	1.0	4.0	-	-
SNARRC- Bs-YC2017	53.1	18.4	14.3	2.0	4.1	1.0	1.0	-	6.1	-	-
SNARRC- Bs-YC2018	48.0	22.5	8.2	1.0	6.1	5.1	5.1	4.1	-	-	-
SNARRC- Bs-YC2019	54.2	21.9	4.2	1.0	11.5	1.0	3.1	1.0	2.1	-	-
Los Lunas-Bs- ABP18-4WI	41.9	25.7	12.5	0.7	9.6	0.7	2.2	2.2	4.4	-	0.7
2021 ABQ BioPark-Bs-YC16	51.0	25.5	5.1	2.0	7.1	-	4.1	2.0	3.1	-	-
2021 ABQ BioPark-Bs-YC19	46.2	20.6	12.6	1.0	6.0	2.0	3.0	1.5	6.5	-	0.5
2021 ABQ BioPark-Bs-YC20	42.2	30.6	10.9	-	6.2	0.8	1.2	0.8	6.6	0.4	0.4
2021_SNARRC- Bs_YC20	40.7	30.2	7.5	0.5	11.6	0.5	2.5	0.5	5.0	-	1.0
2021 LLSMR-Bs-YC19	34.0	26.0	10.0	-	10.0	4.0	2.0	4.0	10.0	-	-
2021 LLSMR-Bs-YC20	47.0	24.8	7.4	1.3	5.4	0.7	1.3	4.7	7.4	-	-